Computational and Theoretical Chemistry 1082 (2016) 41–48

Contents lists available at ScienceDirect

Computational and Theoretical Chemistry

journal homepage: www.elsevier.com/locate/comptc

Anisotropy effect of multi-center Lennard-Jones molecular clusters

Rui Gong, Longjiu Cheng *

Department of Chemistry, Anhui University, Hefei, Auhui 230039, People's Republic of China

ARTICLE INFO

Article history:
Received 28 February 2016
Received in revised form 7 March 2016
Accepted 8 March 2016
Available online 10 March 2016

Keywords:
Anisotropy
Structural optimization
Multi-center Lennard-Jones potential
Atomic clusters

ABSTRACT

Models of randomly packed hard molecules of Multi-Center Lennard-Jones (MCLJ) clusters exhibit some features of anisotropy effects. To investigate the anisotropy effect on the structures of molecular clusters, four highly symmetrical molecules are modeled: 4-atom tetrahedron (TLJ), 6-atom octahedron (OLJ), 8-atom cube (CLJ), and 12-atom icosahedron (ILJ). The intermolecular interactions are described using the MCLJ model. Using the funnel hopping algorithm, we located the putative global minimum structures of these four MCLJ molecular clusters up to cluster size $N = 80$. The structural patterns of these MCLJ clusters are much different to that of Lennard-Jones clusters, and some new rules and structures are found. The structures of TLJ clusters are most irregular due to the highest anisotropy effect of the tetrahedral molecule. For OLJ clusters, a new structural pattern, rhombic dodecahedron, is viewed. The structures of CLJ clusters are also interesting, which look like oblique face-centered cubic (fcc) structures. For ILJ clusters, icosahedral motifs are favored at cluster size $N \leqslant 19$, and fcc motifs are favored more at $N > 19$.

1. Introduction

Random packing problems of rigid geometries have been studied by biologists, materials scientists, engineers, chemists, and physicists to understand the structure of living cells, liquids, granular media, glasses, and amorphous solids [1–5]. A variety of geometries who are packed are paid attention to, for examples spheres and spherocylinders [6–9]. In the field of chemistry, packing of polygons, molecule and atom are most favored. Such as packing of C_6H_6, C_{60}, Au, ethane and methane [10–14]. Random packing problems of identical spheres are the largest number of studies. To study the packing of spheres, some models are used, such as Lennard-Jones (LJ) model.

LJ clusters represent one such test system. It is often used to simulate atomic clusters, especially for rare gas atomic clusters [15–18]. It also plays an important role in studying the nonbonding pair interactions in many complex molecular systems. Here the LJ pair potential is

$$E_{LJ}(r) = \varepsilon\left[\left(\frac{r_0}{r_{ij}}\right)^{12} - 2\left(\frac{r_0}{r_{ij}}\right)^{6}\right], \quad (1)$$

where r_0 is the equilibrium pair separation between two atoms, ε is the pair equilibrium well depth, $\varepsilon = 1$, is used in this work. The LJ model is obviously simple to implement, and their optimal structures display a very regular variation [19,20]. Icosahedral motifs are most favored for LJ clusters, and only at some magic numbers, decahedral, face-centered cubic (fcc), and tetrahedral motifs can be global minima. For example, LJ_{38} is fcc; LJ_{98} has tetrahedral symmetry [21].

As a simple model, LJ model is important in the study of multi-center LJ (MCLJ) molecular clusters. For C_{60} molecular clusters with all-atom potential [11], the intermolecular interaction between C_{60} molecules is nearly the sum of C–C LJ interactions between two molecules. This kind of C_{60}–C_{60} interaction is somewhat a MCLJ model where realistic molecular anisotropy is considered. The favorite structures are much different from those of the LJ potential, where decahedral and close-packed motifs are more favored for C_{60} molecular clusters [22,23]. Two-center Lennard-Jones (2CLJ) model is a special MCLJ model. The ratio of the diatomic bond length to the LJ equilibrium length is varied to increase the degree of anisotropy [24]. Large ratio means strong anisotropy effect. With the increase of anisotropy effect, the potential range increases at optimal orientation, and the global minima change from icosahedral, to polyicosahedral and to novel irregular structures.

The research of the packing of highly symmetrical molecules is of fundamental interests. In this work, four highly symmetrical molecules, tetrahedron, octahedron, cube, and icosahedron, are modeled. The intermolecular interactions are described using the MCLJ model. Given the general importance of the LJ cluster as a simple model cluster, MCLJ model can provide a straightforward analysis of the effect of molecular shape on the structures of

* Corresponding author.
E-mail address: clj@ustc.edu (L. Cheng).

http://dx.doi.org/10.1016/j.comptc.2016.03.008
2210-271X/

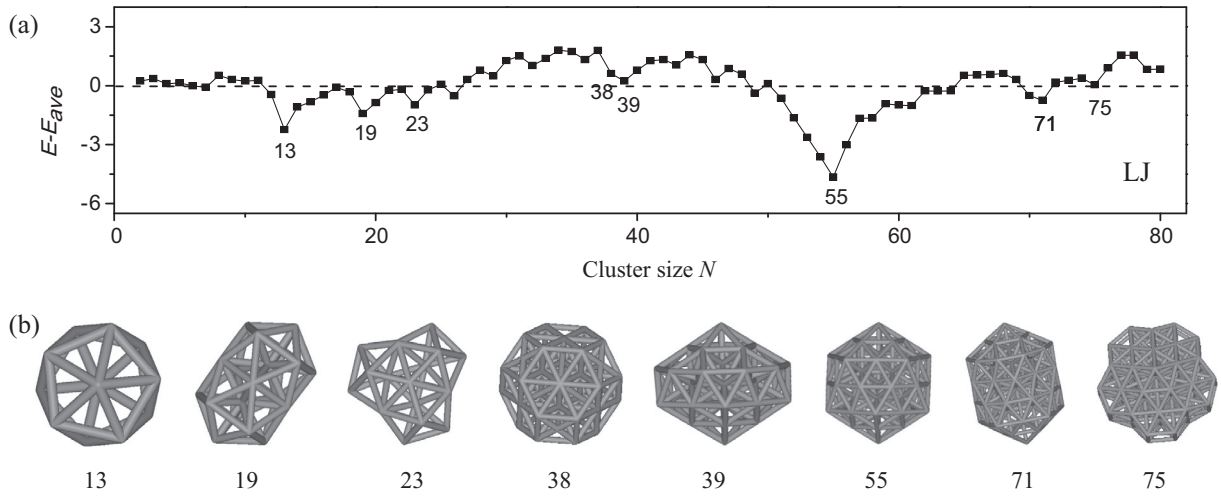

Fig. 1. (a) Plots of the relative energies of the global minima of LJ clusters as a function of cluster size $2 \leqslant N \leqslant 80$. E is the energy of the global minima, and Eave is a four-parameter fit to the global minima energy ($E_{ave} = aN + bN^{2/3} + cN^{1/3} + d$) Downward peaks represent the most stable magic numbers compared to the neighbors. (b) Geometries of most stable magic numbers.

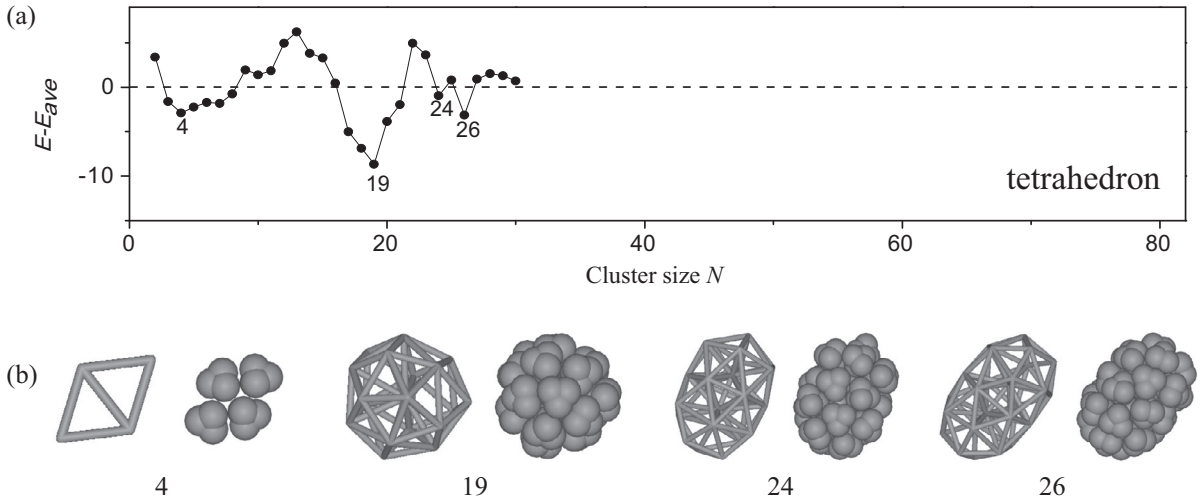

Fig. 2. (a) Plots of the relative energies of the global minima of TLJ clusters as a function of cluster size $2 \leqslant N \leqslant 30$. (b) Geometries of most stable magic numbers. For each cluster size, the structures on the left show an overall view of the cluster (each ball means the mass center of each molecule) and those on the right show the real molecular clusters.

clusters. The potential energy surfaces of MCLJ clusters are more rugged than that of LJ cluster, so the highly efficient "funnel hopping" algorithm [25] is employed to carry out this searching on the potential energy surfaces.

2. Method

2.1. MCLJ model

MCLJ model is important in physics. In this work, as a model study and for simplicity, each molecule is treated as a rigid body and only the LJ interactions are considered. Using the MCLJ model, the energy between two molecules can be written as:

$$E(\alpha,\beta) = \sum_{i=1}^{N}\sum_{j=1}^{N} E_{LJ}(r_{ij}^{\alpha\beta}) \tag{2}$$

where N is the number of atoms in a molecule, and $r_{ij}^{\alpha\beta}$ is the distance between atom i of molecule α and atom j of molecule β. Tetrahedron, octahedron, cube and icosahedron are studied here since they are highly symmetrical polyhedron models. Clusters of 4-atom tetrahedral molecules are called tetrahedral Lennard-Jones (TLJ) clusters; accordingly, clusters of 6-atom octahedral, 8-atom cubic and 12-atom icosahedral molecules are called octahedral Lennard-Jones (OLJ), cubic Lennard-Jones (CLJ) and icosahedral Lennard-Jones (ILJ) clusters, respectively. In this model study, the bond length in each molecule is set to $0.45r_0$, which is in agreement with the ratio of covalent and van der Waals radius of carbon.

2.2. "Funnel hopping" algorithm

Because of the enormous number of local minimum structures of atomic and molecular clusters, it is difficult to locate the lowest energy conformation in the fields of chemistry. The global optimization algorithm [26–32] has been widely used to locate global minimum structures. In the past years, a variety of methods have been developed for global structural prediction, such as "Funnel hopping" algorithm, simulated annealing algorithm [33,34], genetic algorithm (GA) [35,36], basin-hopping and its variants [37,38], particle swarm optimization [39,40], random tunneling

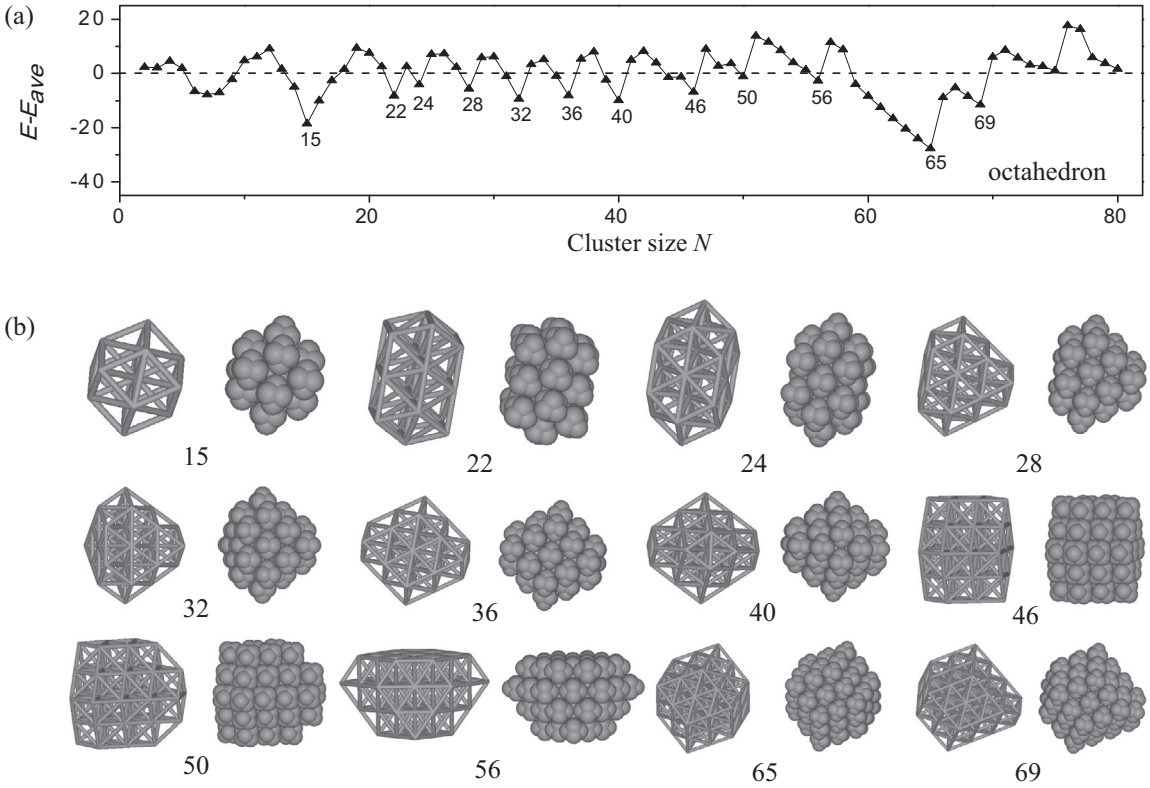

Fig. 3. (a) Plots of the relative energies of the global minima of OLJ clusters as a function of cluster size $2 \leqslant N \leqslant 80$. (b) Geometries of most stable magic numbers.

algorithm [41–43], potential deformation [44,45], simple linkage [46,47], and modeling methods [48–50] and so on. "Funnel hopping" algorithm is used to locate global minimum structures in this work.

"Funnel hopping" algorithm is an unbiased global optimization method, it is used to locate the global minimum structures of the MCLJ clusters. The basic idea of this algorithm is to insert a second local optimization phase between the first gradient-based local optimization phase and the global optimization phase. The goal of the second local optimization phase is to locate the minimum of the funnel that contains current configuration in the energy landscape with the least cost. Then the global optimization phase can focus on the global information of the potential energy surface over the various funnels. The first local optimization phase is performed with the limited memory quasi-Newton method [51]. The method is a highly effective method of local optimization. Then, using cluster surface smoothing method to make the second local optimization. Cluster surface smoothing method is similar to the dynamic lattice searching method [52], which can smooth the cluster surface by optimizing the approximate lattice. The global optimization is a simple version of genetic algorithm [53–55]. This "funnel hopping" algorithm is effective for structure optimization of atomic and molecular clusters.

3. Results and discussion

For TLJ clusters, it is difficult to optimize the structures, so we only obtained the global minimum structures up to $N = 30$. For other MCLJ clusters, we obtained the putative global minimum structures up to $N = 80$. For each cluster size, ten separate runs are performed, and for each run 5000 hoppings are carried out.

As a comparison, Fig. 1 gives the energy sequences of the global minima of LJ clusters in a manner that emphasizes particular stable minima or "magic numbers", where data of LJ clusters are from the Cambridge Cluster Database [56]. E is the energy of the global minima, and E_{ave} is a four-parameter fit to the global minima energy ($E_{ave} = aN + bN^{2/3} + cN^{1/3} + d$). Downward peaks represent the most stable magic numbers compared to the neighbors. The magic number and typical structures are also given in this figure, where icosahedral and polyicosahedral motifs are most favored [15].

3.1. Packing of tetrahedron

When the molecular shape is tetrahedron (Fig. 2), we have only located the optimal structures up to 30 considering the rugged potential energy surface. Compared with the energy sequence of LJ, the energy sequence of tetrahedron molecular cluster are much different. The magic numbers are $N = 4$, 19, 24, and 26. As shown in Fig. 2(b), the structures are irregular. TLJ_4 is a parallelogram and with C_{2h} symmetry. TLJ_{19} is a particular stable structure with one molecule in the center and others surrounding it, but the structure is chaotic in C_1 symmetry. TLJ_{24} and TLJ_{26} are two molecules in the center and others surrounding them, both of them are in C_3 symmetry.

Methane clusters have been investigated by Takeuchi [57], which is a system in real work similar to the TLJ model. By comparison, we found that the structural pattern of methane clusters are similar to that TLJ clusters. For small methane clusters, those with $N = 10$, 15, 19, 22, 24 are relatively more stable, where TLJ_{19} and TLJ_{24} are similar to $(CH_4)_{19}$ and $(CH_4)_{24}$, respectively.

3.2. Packing of octahedron

As shown in Fig. 3(a), the energy sequence of OLJ clusters is also much different from that of LJ clusters. The most stable magic numbers are $N = 15$, 22, 24, 28, 32, 36, 40, 46, 50, 56, 65, and 69. The sequence of magic number seems to contain some rule, especially from 24 to 40 with an increment of 4.

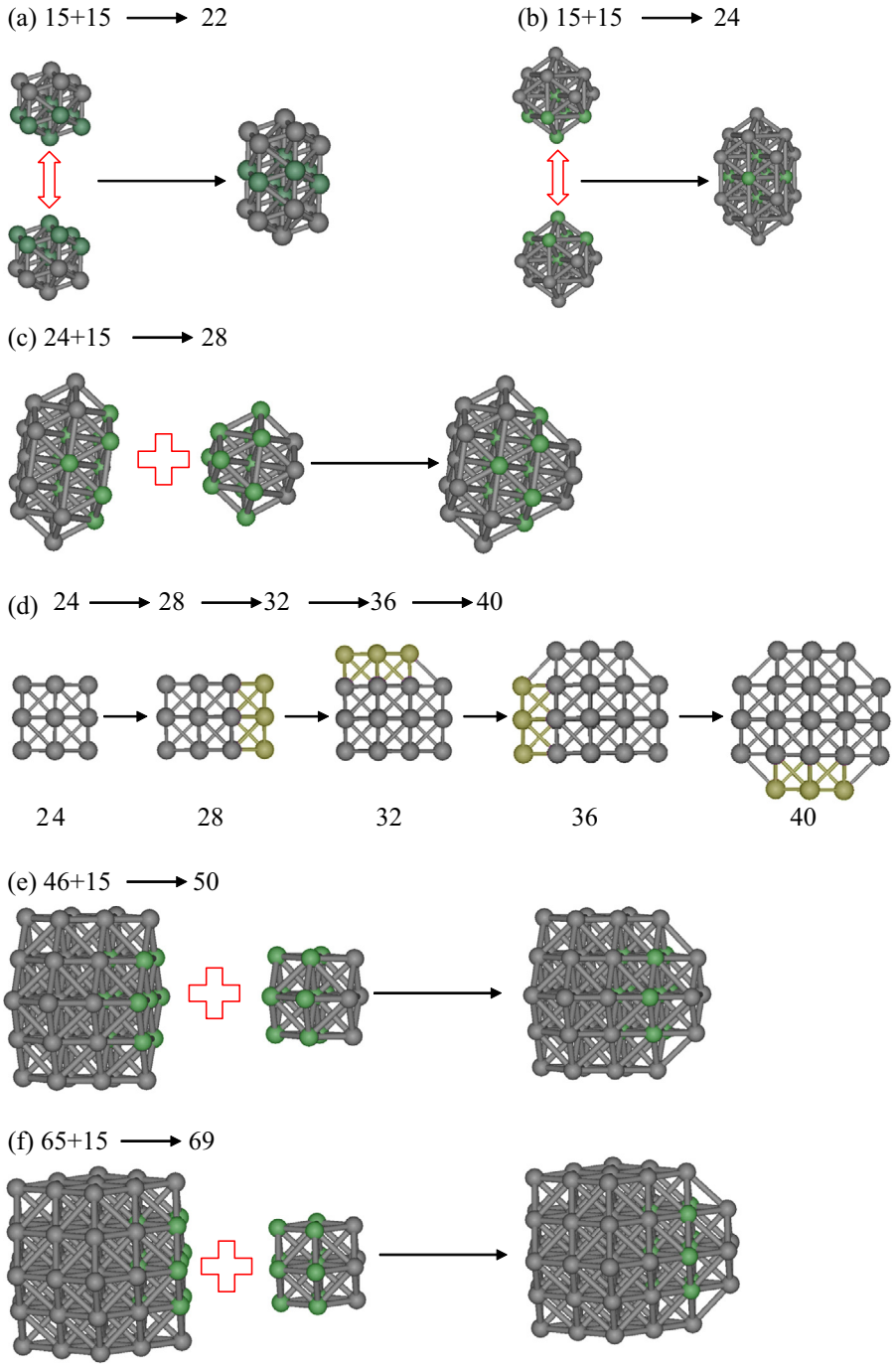

Fig. 4. The evolution law of typical structures of OLJ clusters. Green balls are shared part of two structures, and yellow balls are the added part. (For interpretation of the references to color in this figure legend, the reader is referred to the web version of this article.)

Fig. 3(b) plots the magic number and typical structures of OLJ clusters. Compared with LJ clusters, icosahedral, fcc, and decahedral motifs are not the global minimum structures of OLJ clusters. Instead, a new structural pattern, rhombic dodecahedron, is viewed. Rhombic dodecahedron has 14 vertices, 24 equal edges and 12 identical rhombic surfaces.

OLJ_{15} is a simple rhombic dodecahedron with a complete shell. It has one central molecule and 12 rhombic faces. The 14 vertices can be classified in two groups: 6 vertices at the acute angle of the rhombic faces and 8 vertices at the obtuse angle of the rhombic faces. The distances from the center to the two kinds of vertices are not identical (1:1.15).

Rhombic dodecahedron is a new packing not viewed in other clusters. OLJ_{15} and OLJ_{65} are rhombic dodecahedra with complete shells. As shown in Fig. 4, the other global minimum structures of OLJ clusters are also rhombic dodecahedron. OLJ_{22} and OLJ_{24} are both formed of two OLJ_{15} (Fig. 4a and b). The rule of the sequence of magic numbers from 24 to 40 is illustrated in Fig. 4c and d. OLJ_{46} and OLJ_{56} are formed of several OLJ_{15}, and the other structures are also formed of several small OLJ clusters.

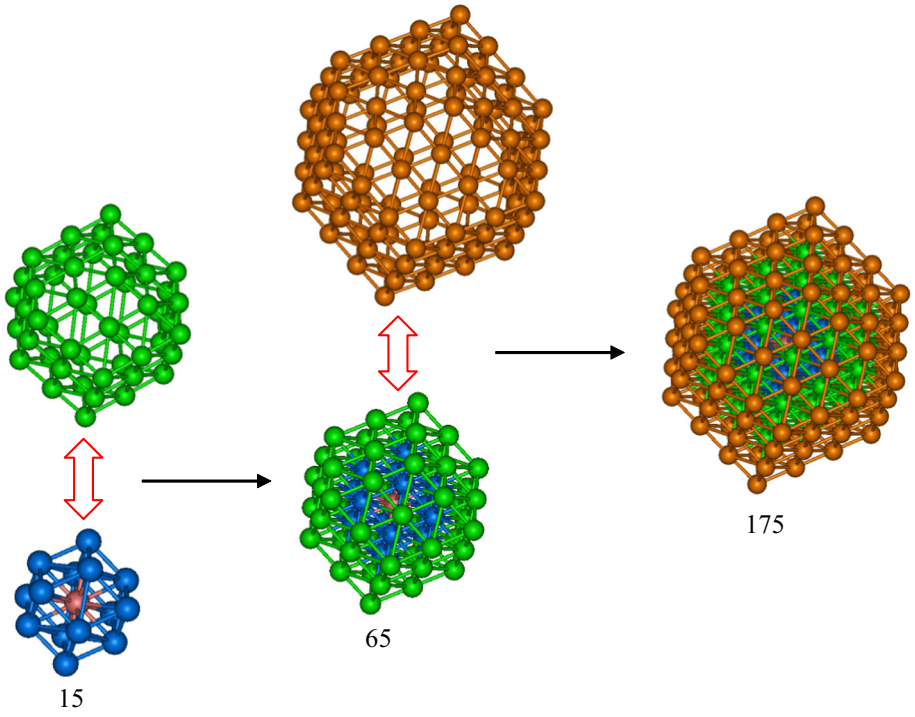

Fig. 5. The evolution between OLJ_{15}, OLJ_{65} and OLJ_{175} clusters. Each OLJ molecule is represented as a ball showing in different colors with different layers. (For interpretation of the references to colour in this figure legend, the reader is referred to the web version of this article.)

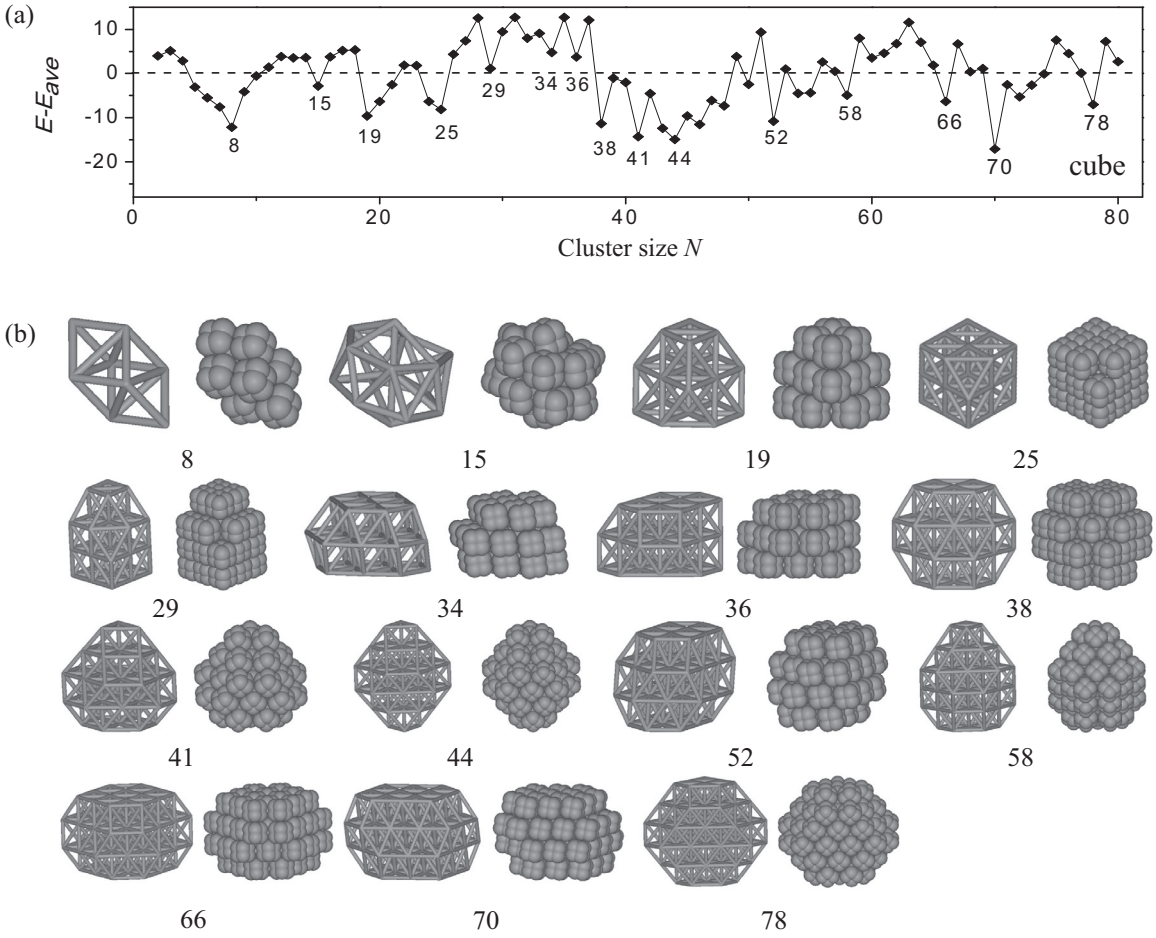

Fig. 6. (a) Plots of the relative energies of the global minima of CLJ clusters as a function of cluster size $2 \leqslant N \leqslant 80$. (b) Geometries of most stable magic numbers.

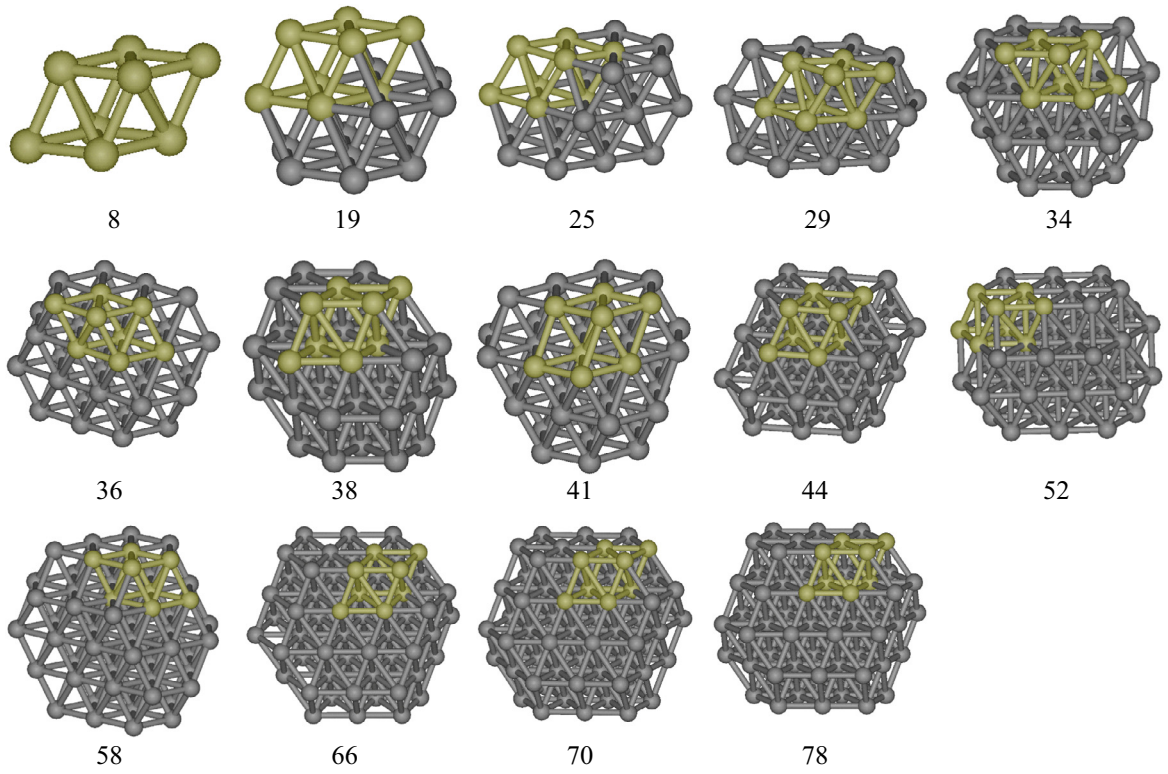

Fig. 7. The global minima of CLJ clusters built upon the unit cell. The yellow part is the unit cell. (For interpretation of the references to colour in this figure legend, the reader is referred to the web version of this article.)

It is well known that LJ_{13}, LJ_{55} and LJ_{147} are magic numbers of icosahedra: LJ_{13} is one-layer; LJ_{55} is two-layer; LJ_{147} is three-layer [58]. Interestingly, OLJ_{15}, OLJ_{65} and OLJ_{175} follow similar rule of multiple layers. According to rhombic dodecahedron with complete shells (OLJ_{15} and OLJ_{65}), we constructed the next magic number of rhombic dodecahedron, OLJ_{175}. Fig. 5 shows the relationship between the three structures. OLJ_{65} is OLJ_{15} plus a rhombic dodecahedral overlayer, and OLJ_{175} is OLJ_{65} plus a bigger rhombic dodecahedral overlayer.

3.3. Packing of cube

As shown in Fig. 6(a), the energy sequence of CLJ clusters is different from that of LJ clusters too. The magic number is $N = 8$, 15, 19, 25, 29, 34, 36, 38, 41, 44, 52, 58, 66, 70 and 78.

Fig. 6(b) plots the magic number and typical structures of CLJ clusters. CLJ_{15} is a particular stable structure in C_1 symmetry, which is a distortion of the global minimum structure of Morse clusters [59]. Except for CLJ_{15}, other magic numbers are in regular packing, which is a deformation of fcc. The structures both have a unit cell of OLJ_8, which is a parallelepiped with 6 identical rhombic surfaces (the acute angle of the rhombic is 69.5°). The unit cell is oblique, and the structures are a kind of oblique fcc.

Fig. 7 plots these structures and their unit cell. It is found that each structure can be obtained by translating the unit cells. CLJ_8 is one unit cell, which is a parallelepiped in D_{3d} symmetry. When CLJ_8 move along the shorter diagonal line and side of rhombic surfaces, other typical structures can be obtained. CLJ_{19} is a simple example, which is the union of three CLJ_8. Similarly, CLJ_{25} are generated by translating unit cell five times, and CLJ_{29} by seven times. With cluster size increasing, the structures are more complex, but it still follow the rule.

3.4. Packing of icosahedron

Fig. 8 plots the energy sequence and most stable magic numbers of ILJ clusters. At $N \leqslant 19$, the global minimum structures of ILJ clusters are icosahedral packing similar to those of LJ clusters. ILJ_{13} and ILJ_{19} are two most stable magic numbers in icosahedral packing. However, at $N > 19$, the global minimum structures are in fcc packing with magic numbers $N = 24$, 38, 52, 61, 63, 68, 70 and 78. Among which, ILJ_{38} is a perfect fcc truncated octahedron, which is also the global minimum structure of LJ clusters.

The 12-atom icosahedral molecule is the most spherical in the four model molecules, and it is close to C_{60} molecule in shape. The sequences of the global minimum structures of ILJ and C_{60} clusters are similar at small sizes, where icosahedral motifs are favored more. At large cluster sizes, icosahedral motifs are too strained and the fcc, hexagonal close packed (hcp), and decahedral motifs are favored more for C_{60} clusters [22,23,60,61]. However, the hcp and decahedral motifs are not viewed in ILJ clusters and only the fcc motifs are favored.

3.5. Anisotropy effect of the molecules

For the four highly symmetrical model molecules in this work, the molecule is anisotropic in shape, and the anisotropy effect has great influence on the packing of the clusters of molecules. TLJ molecule is of the highest anisotropy effect, and there is no particular packing of clusters satisfying the symmetry of molecule, so the TLJ clusters are in irregular packing. For OLJ and CLJ clusters, the rhombic dodecahedral and oblique fcc packings match the orientation of molecules, respectively.

It was well studied that, for pair potentials without anisotropy effect, potential range is the key factor determining the favorite

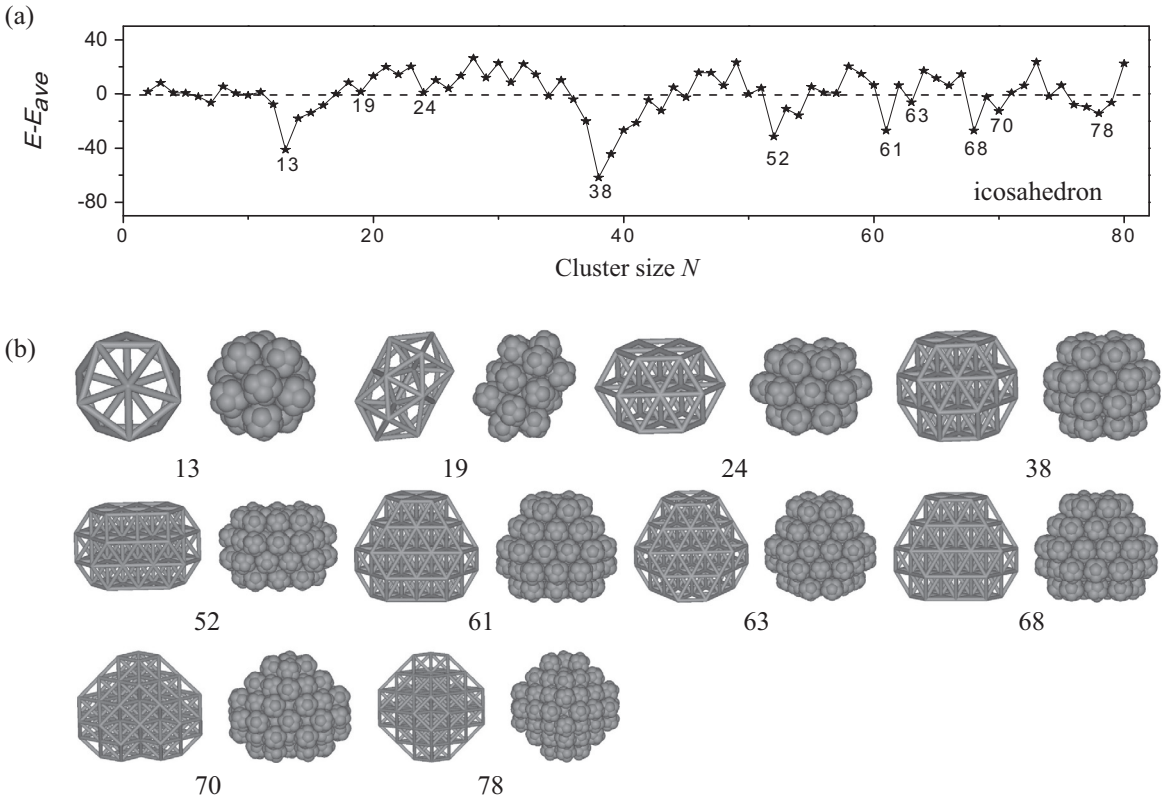

Fig. 8. (a) Plots of the relative energies of the global minima of ILJ clusters as a function of cluster size $2 \leqslant N \leqslant 80$. (b) Geometries of most stable magic numbers.

packing of clusters. For Morse potential [62] with changeable pair potential range, disordered and polyicosahedral packings are favored by clusters with long-ranged pair potentials, icosahedral packing is favored at the middle-ranged pair potential, and fcc, hcp, and decahedral packings are favored at the short-ranged potentials [63–66]. However, the rhombic dodecahedral and oblique fcc packings are not viewed in any clusters with isotropic potentials, which are unique resulting from anisotropy effect of the molecules.

For the highly spherical C_{60} molecule, anisotropy effect is insignificant, and the global minimum cluster structures of anisotropic all-atom MCLJ potential [11] do not differ greatly from those of isotropic Girifalco [67] and PPR potentials [68], which are similar to those of short-ranged Morse potentials [65]. The sequences of global minimum structures of ILJ clusters is similar to those of C_{60} clusters, indicating certain isotropic feature of the pair potential. However, anisotropy effect is also obvious for ILJ clusters, of which only fcc packing is favored at large cluster size and the most stable magic numbers of hcp and decahedral packings viewed in C_{60} and short-ranged Morse clusters are even not the global minimum ones.

4. Conclusions

In summary, to study the anisotropy effect on the structures of molecular clusters, we modeled for high-symmetry molecules: 4-atom tetrahedron (TLJ), 6-atom octahedron (OLJ), 8-atom cube (CLJ), and 12-atom icosahedron (ILJ). Only the LJ interactions are concerned for the intermolecular interactions described by the MCLJ model. The global minimum structures of these four model molecular clusters up to cluster size $N = 80$ were located by funnel-hopping method. The sequences of the global minimum structures of these four MCLJ clusters differ greatly to that of LJ clusters due to the anisotropy effect. The TLJ molecule is the most anisotropic in the four model molecules, and the global minimum structures are irregular. For OLJ clusters, a new packing, rhombic dodecahedron, are favored in energy. Similar to icosahedron, rhombic dodecahedron also has onion-like layered structures with magic numbers $N = 15$, 65, and 175. For CLJ clusters, the global minimum structures are oblique fcc with a CLJ_8 unit. For icosahedron molecular clusters, icosahedron and fcc motifs are most favored. The anisotropy effect of the MCLJ molecules results in the rhombic dodecahedral and oblique fcc packings, which are novel and not viewed in clusters with isotropic potentials. The global minimum structures of ILJ clusters agree with the ones of C_{60} and short-ranged Morse clusters at small sizes, where the global minima are icosahedral. However, only fcc packing is favored at large cluster size of ILJ clusters, which is different from those of C_{60} and short-ranged Morse clusters where hcp and decahedral packings are also favored. It is well studied that the potential range is a key factor determining the favorite packing of clusters. Packing of rigid molecules is of fundamental interests. MCLJ model is relatively simple, and our results clearly present the anisotropy effect on the structures of MCLJ clusters. These results provide further information about the anisotropic systems and it is expected to offer a useful pointer to the anisotropic systems in a real physical world.

Acknowledgements

This work is supported by the National Natural Science Foundation of China (21273008, 21573001). The calculations are carried out on the High-Performance Computing Centre of Anhui University.

References

[1] S. Torquato, T.M. Truskett, P.G. Debenedetti, Is random close packing of spheres well defined?, Phys Rev. Lett. 84 (2000) 2064.
[2] C.S. O'Hern, S.A. Langer, A.J. Liu, S.R. Nagel, Random packings of frictionless particles, Phys. Rev. Lett. 88 (2002) 075507.
[3] S. Williams, A. Philipse, Random packings of spheres and spherocylinders simulated by mechanical contraction, Phys. Rev. E 67 (2003) 051301.
[4] A. Donev, I. Cisse, D. Sachs, E.A. Variano, F.H. Stillinger, R. Connelly, S. Torquato, P.M. Chaikin, Improving the density of jammed disordered packings using ellipsoids, Science 303 (2004) 990–993.
[5] T. Aste, M. Saadatfar, T. Senden, Geometrical structure of disordered sphere packings, Phys. Rev. E 71 (2005) 061302.
[6] J.G. Berryman, Random close packing of hard spheres and disks, Phys. Rev. A 27 (1983) 1053.
[7] W. Jodrey, E. Tory, Computer simulation of close random packing of equal spheres, Phys. Rev. A 32 (1985) 2347.
[8] V.N. Manoharan, M.T. Elsesser, D.J. Pine, Dense packing and symmetry in small clusters of microspheres, Science 301 (2003) 483–487.
[9] J. Zhao, S. Li, R. Zou, A. Yu, Dense random packings of spherocylinders, Soft Matter 8 (2012) 1003–1009.
[10] R.F. Cracknell, D. Nicholson, N. Quirke, A grand canonical Monte-Carlo study of Lennard-Jones mixtures in slit pores; 2: mixtures of two centre ethane with methane, Mol. Simul. 13 (1994) 161–175.
[11] J.P. Doye, A. Dullweber, D.J. Wales, Structural predictions for $(C_{60})_N$ clusters with an all-atom potential, Chem. Phys. Lett. 269 (1997) 408–412.
[12] J. Li, X. Li, H.-J. Zhai, L.-S. Wang, Au_{20}: A tetrahedral cluster, Science 299 (2003) 864–867.
[13] O. Adisa, B. Cox, J. Hill, Packing configurations for methane storage in carbon nanotubes, Eur. Phys. J. B 79 (2011) 177–184.
[14] H. Takeuchi, Structural features of small benzene clusters $(C_6H_6)_n$ ($n \leqslant 30$) as investigated with the all-atom OPLS potential, J. Phys. Chem. A 116 (2012) 10172–10181.
[15] J. Lennard-Jones, On the forces between atoms and ions, Royal Society (1925) 584–597.
[16] W. Cai, Y. Feng, X. Shao, Z. Pan, Optimization of Lennard-Jones atomic clusters, J. Mol. Struct. 579 (2002) 229–234.
[17] E.G. Noya, J.P. Doye, Structural transitions in the 309-atom magic number Lennard-Jones cluster, J. Chem. Phys. 124 (2006) 104503.
[18] X. Yang, W. Cai, X. Shao, A dynamic lattice searching method with constructed core for optimization of large lennard-jones clusters, J. Comput. Chem. 28 (2007) 1427–1433.
[19] J.P. Doye, L. Meyer, Mapping the magic numbers in binary Lennard-Jones clusters, Phys. Rev. Lett. 95 (2005) 063401.
[20] D. Sabo, J. Doll, D.L. Freeman, Taming the rugged landscape: production, reordering, and stabilization of selected cluster inherent structures in the $X_{13-n}Y_n$ system, J. Chem. Phys. 121 (2004) 847–855.
[21] R.H. Leary, J.P. Doye, Tetrahedral global minimum for the 98-atom Lennard-Jones cluster, Phys. Rev. E 60 (1999) R6320.
[22] J.P. Doye, D.J. Wales, W. Branz, F. Calvo, Modeling the structure of clusters of C_{60} molecules, Phys. Rev. B 64 (2001) 235409.
[23] L. Cheng, W. Cai, X. Shao, Geometry optimization and conformational analysis of (C60)N clusters using a dynamic lattice-searching method, ChemPhysChem 6 (2005) 261–266.
[24] Y. Feng, J. Wu, L. Cheng, H. Liu, Anisotropy effect on global minimum structures of clusters: two-center Lennard-Jones model, J. Chem. Phys. 135 (2011) 244108.
[25] L. Cheng, Y. Feng, J. Yang, J. Yang, Funnel hopping: Searching the cluster potential energy surface over the funnels, J. Chem. Phys. 130 (2009) 214112.
[26] D.J. Wales, J.P. Doye, Global optimization by basin-hopping and the lowest energy structures of Lennard-Jones clusters containing up to 110 atoms, J. Phys. Chem. A 101 (1997) 5111–5116.
[27] D.J. Wales, H.A. Scheraga, Global optimization of clusters, crystals, and biomolecules, Science 285 (1999) 1368–1372.
[28] L. Cheng, W. Cai, X. Shao, A connectivity table for cluster similarity checking in the evolutionary optimization method, Chem. Phys. Lett. 389 (2004) 309–314.
[29] C.A. Floudas, C.E. Gounaris, A review of recent advances in global optimization, J. Glob. Optim. 45 (2009) 3–38.
[30] X. Luo, J. Yang, H. Liu, X. Wu, Y. Wang, Y. Ma, S.-H. Wei, X. Gong, H. Xiang, Predicting two-dimensional boron–carbon compounds by the global optimization method, J. Am. Chem. Soc. 133 (2011) 16285–16290.
[31] H.-Z. Chen, Y.-Y. Zhang, X. Gong, H. Xiang, Predicting new TiO_2 phases with low band gaps by a multiobjective global optimization approach, J. Phys. Chem. C 118 (2014) 2333–2337.
[32] Q. Zhang, L. Cheng, Structural determination of $(Al_2O_3)_n$ (n = 1–15) clusters based on Graphic Processing Unit, J. Chem. Inf. Model. (2015).
[33] B. Sankararao, C.K. Yoo, Development of a robust multiobjective simulated annealing algorithm for solving multiobjective optimization problems, Ind. Eng. Chem. Res. 50 (2011) 6728–6742.
[34] R.Q. Topper, W.V. Feldmann, I.M. Markus, D. Bergin, P.R. Sweeney, Simulated annealing and density functional theory calculations of structural and energetic properties of the ammonium chloride clusters $(NH_4Cl)_n$,$(NH_4^+)(NH_4Cl)_n$, and $(Cl^-)(NH_4Cl)_n$, n = 1–13, J. Phys. Chem. 115 (2011) 10423–10432.
[35] A.N. Alexandrova, $H\cdot(H_2O)_n$ clusters: microsolvation of the hydrogen atom via molecular ab initio gradient embedded genetic algorithm (GEGA), J. Phys. Chem. A 114 (2010) 12591–12599.
[36] M.X. Silva, B.R. Galvão, J.C. Belchior, Theoretical study of small sodium–potassium alloy clusters through genetic algorithm and quantum chemical calculations, Phys. Chem. Chem. Phys. 16 (2014) 8895–8904.
[37] H. Do, N.A. Besley, Structural optimization of molecular clusters with density functional theory combined with basin hopping, J. Chem. Phys. 137 (2012) 134106.
[38] Y.-R. Liu, H. Wen, T. Huang, X.-X. Lin, Y.-B. Gai, C.-J. Hu, W.-J. Zhang, W. Huang, Structural exploration of water, nitrate/water, and oxalate/water clusters with basin-hopping method using a compressed sampling technique, J. Phys. Chem. A 118 (2014) 508–516.
[39] J. Kennedy, Particle Swarm Optimization, Encyclopedia of Machine Learning, Springer, 2010, pp. 760–766.
[40] Y. Wang, B. Li, T. Weise, J. Wang, B. Yuan, Q. Tian, Self-adaptive learning based particle swarm optimization, Inf. Sci. 181 (2011) 4515–4538.
[41] H. Jiang, W. Cai, X. Shao, A random tunneling algorithm for the structural optimization problem, Phys. Chem. Chem. Phys. 4 (2002) 4782–4788.
[42] X. Shao, H. Jiang, W. Cai, Parallel random tunneling algorithm for structural optimization of Lennard-Jones clusters up to n= 330, J. Chem. Inf. Comput. Sci. 44 (2004) 193–199.
[43] A.Y. Gornov, T.S. Zarodnyuk, Tunneling algorithm for solving nonconvex optimal control problems, Optimization, Simulation, and Control, Springer, 2013, pp. 289–299.
[44] L. Piela, J. Kostrowicki, H.A. Scheraga, On the multiple-minima problem in the conformational analysis of molecules: deformation of the potential energy hypersurface by the diffusion equation method, J. Phys. Chem. 93 (1989) 3339–3346.
[45] K. Kaasbjerg, K.S. Thygesen, A.-P. Jauho, Acoustic phonon limited mobility in two-dimensional semiconductors: Deformation potential and piezoelectric scattering in monolayer MoS_2 from first principles, Phys. Rev. B 87 (2013) 235312.
[46] M. Locatelli, F. Schoen, Simple linkage: analysis of a threshold-accepting global optimization method, J. Glob. Optim. 9 (1996) 95–111.
[47] M. Lorieux, MapDisto: fast and efficient computation of genetic linkage maps, Mol. Breed. 30 (2012) 1231–1235.
[48] J. Northby, Structure and binding of Lennard-Jones clusters: 13$\leqslant$ N$\leqslant$ 147, J. Chem. Phys. 87 (1987) 6166–6177.
[49] D. Romero, C. Barrón, S. Gómez, The optimal geometry of Lennard-Jones clusters: 148–309, Comput. Phys. Commun. 123 (1999) 87–96.
[50] G. Li, J. Shi, X. Qu, Modeling methods for GenCo bidding strategy optimization in the liberalized electricity spot market – a state-of-the-art review, Energy 36 (2011) 4686–4700.
[51] D.C. Liu, J. Nocedal, On the limited memory BFGS method for large scale optimization, Math. Program. 45 (1989) 503–528.
[52] X. Shao, L. Cheng, W. Cai, A dynamic lattice searching method for fast optimization of Lennard-Jones clusters, J. Comput. Chem. 25 (2004) 1693–1698.
[53] D. Deaven, K. Ho, Molecular geometry optimization with a genetic algorithm, Phys. Rev. Lett. 75 (1995) 288.
[54] B. Hartke, Global cluster geometry optimization by a phenotype algorithm with Niches: location of elusive minima, and low-order scaling with cluster size, J. Comput. Chem. 20 (1999) 1752–1759.
[55] R.L. Johnston, Evolving better nanoparticles: genetic algorithms for optimising cluster geometries, Dalton Trans. (2003) 4193–4207.
[56] E. Yurtsever, F. Calvo, D. Wales, Finite-size effects in the dynamics and thermodynamics of two-dimensional Coulomb clusters, Phys. Rev. E 72 (2005) 026110.
[57] H. Takeuchi, The structural investigation on small methane clusters described by two different potentials, Comput. Theor. Chem. 986 (2012) 48–56.
[58] L. Cheng, J. Yang, Global minimum structures of morse clusters as a function of the range of the potential: 81$\leqslant$ n$\leqslant$ 160, J. Phys. Chem. A 111 (2007) 5287–5293.
[59] J. Wu, L. Cheng, Global minimum structures and structural phase diagrams of modified Morse clusters: 11$\leqslant$ N$\leqslant$ 30, J. Chem. Phys. 134 (2011) 194108.
[60] C. Rey, L. Gallego, J. Alonso, Molecular-dynamics study of the structure, binding energy, and melting of small clusters of fullerene molecules using Girifalco's spherical model, Phys. Rev. B 49 (1994) 8491.
[61] J.P. Doye, D.J. Wales, The structure of $(C_{60})_N$ clusters, Chem. Phys. Lett. 262 (1996) 167–174.
[62] P.M. Morse, Diatomic molecules according to the wave mechanics. II. vibrational levels, Phys. Rev. 34 (1929) 57.
[63] M.A. Miller, J.P. Doye, D.J. Wales, Structural relaxation in Morse clusters: energy landscapes, J. Chem. Phys. 110 (1999) 328–334.
[64] B. Smirnov, A.Y. Strizhev, R. Berry, Structures of large Morse clusters, J. Chem. Phys. 110 (1999) 7412–7420.
[65] L. Cheng, J. Yang, Modified Morse potential for unification of the pair interactions, J. Chem. Phys. 127 (2007) 124104.
[66] Y. Feng, L. Cheng, H. Liu, Putative global minimum structures of Morse clusters as a function of the range of the potential: 161$\leqslant$ n$\leqslant$ 240, J. Phys. Chem. A 113 (2009) 13651–13655.
[67] L. Girifalco, Molecular properties of fullerene in the gas and solid phases, J. Phys. Chem. 96 (1992) 858–861.
[68] J. Pacheco, J.P. Ramalho, First-principles determination of the dispersion interaction between fullerenes and their intermolecular potential, Phys. Rev. Lett. 79 (1997) 3873.